Title

Sarcospan Ameliorates Pathology in D2.mdx Mice, a Severe Model for Duchenne Muscular Dystrophy

Author

Arabatlian, Norayr Levon

Publication Date

2024

Peer reviewed|Thesis/dissertation

UNIVERSITY OF CALIFORNIA

Los Angeles

Sarcospan Ameliorates Pathology in D2.*mdx* Mice, a Severe Model for Duchenne Muscular Dystrophy

A thesis submitted in partial satisfaction of the requirements for the degree Master of Science in Physiological Science

by

Norayr Levon Arabatlian

2024

ABSTRACT OF THE THESIS

Sarcospan Ameliorates Pathology in D2.*mdx* Mice, a Severe Model for Duchenne Muscular Dystrophy

by

Norayr Levon Arabatlian

Master of Science in Physiological Science

University of California, Los Angeles, 2024

Professor Rachelle Hope Crosbie, Chair

Duchenne Muscular Dystrophy (DMD) is a fatal neuromuscular disorder resulting from the loss of dystrophin protein and subsequent loss of the dystrophin-glycoprotein complex (DGC). Although there are new therapeutic options, there still is no cure for the disease. The delay in finding a cure can be partly due to the lack of an appropriate mouse model that recapitulates the pathology seen in DMD patients. Compared to the popular DMD mouse model, B10.*mdx*, the D2.*mdx* murine model presents a more severe muscle disease pathology, more closely matching DMD patients. Our project shows that sarcospan overexpression in D2.*mdx* mice stabilizes the muscle membrane by upregulating the presence of adhesion complex proteins. Sarcospan increases the expression of utrophin, a homolog of dystrophin and a component of the utrophin-glycoprotein complex, compensating for the dystrophin loss in the DGC. Further, quantitative and proteomic analysis reveals an increase in the amount of matrisomal proteins

that supports our hypothesis of an upregulation of adhesion complex proteins in D2.*mdx*^{TG} mice. When examining collagen distribution and abundance changes, we note a restoration of fibrillar collagen solubility, which may account for increased muscle fiber size homogeneity and decreased central nucleation. In conclusion, sarcospan overexpression ameliorates the pathophysiology of the severe mouse model of DMD by strengthening the myofiber membrane and decreasing insoluble collagen linked to fibrosis.

The thesis of Norayr Levon Arabatlian is approved.

Amy Catherine Rowat

Pearl Jennine Quijada

Rachelle Hope Crosbie, Committee Chair

University of California, Los Angeles

2024

DEDICATION

I would like to begin by dedicating this thesis to my mother, Susan Arabatlian, and my late father, Levon Arabatlian. Your unwavering support, guidance, and sacrifices have enabled me to pursue my academic and personal goals. To my late father, I promise to uphold your legacy not only as a diligent worker, but also as a kind and empathetic human being. I would also like to express my gratitude to my twin sister, Leana, who has always encouraged me to take on new challenges and emerge victorious. I dedicate not just this thesis but my entire life to following the values and principles that you have all instilled in me.

Table of Contents

LIST OF FIGURES

ACKNOWLEDGMENTS

I would like to express my gratitude to Dr. Rachelle Crosbie for her constant guidance and support throughout the last two years. She has always been enthusiastic and open to discussions regarding the direction of my paper. I always looked forward to our meetings to absorb as much knowledge as possible. Her encouragement and excitement have provided me with the energy to complete my thesis. My graduate school experience would not have been the same if I didn't have the privilege of being a member of her lab. I would also like to thank my committee members, Dr. Amy Rowat and Dr. Pearl Quijada, for their contributions to my project. Their thorough feedback and general insights as leaders in their respective fields have immensely assisted me with my research.

I would also like to express my gratitude to Dr. Joe Reynolds for his unwavering patience and support. His wisdom and kindness have immensely helped me grow as a researcher. He always motivated me to take up challenging tasks in the lab and guided me through this collaborative project. Thank you for creating a positive and friendly environment in the lab over the years.

Thank you to all current and past members of the Crosbie Lab. Each and every member of the lab has played a significant role in my journey. I appreciate all the feedback and assistance I received for my project. Everyone has influenced my life in numerous ways, and I am deeply grateful for your contagious kindness.

BACKGROUND

Duchenne muscular dystrophy (DMD) is a rare X-linked, fatal degenerative neuromuscular disorder that results from a mutation inherited from the mother's X-chromosome, resulting in the absence of dystrophin (1). DMD is diagnosed in approximately 1 in every 3500 to 5000 males born worldwide (2). The result of DMD is due to a mutation in the 79-exon DMD gene coding for dystrophin, which prevents the production of a functional dystrophin protein. This absence is a vital loss to the dystrophin-glycoprotein complex (DGC), which impedes mechanical stabilization and signaling of cells that mediate interactions between the cytoskeleton and the extracellular matrix (ECM) (3). As a result, most people diagnosed with DMD die by the age of thirty due to cardiac and/or respiratory failure (4).

The lack of an appropriate model to study DMD has hindered researchers' ability to find a more targeted treatment or cure. Thus, finding an accurate model to mimic DMD has been of utmost importance. The most widely used mouse model to study DMD is the B10.*mdx* mouse. There has been debate about whether the B10.*mdx* mouse model is sufficient for replicating the muscle disease. The pathology in the diaphragm mimics the human disease, but the limb muscles lack the histopathology seen in humans. The mild pathology in the limbs and improved muscle regeneration in B10.*mdx* mice compared to humans (5). To have a model that more closely recapitulates the disease phenotype in humans, the D2.*mdx* murine line was generated. Crossing the dystrophin mutation found in the B10.*mdx* mouse with the DBA/2J background results in a mouse model with more severe muscle pathology - D2.*mdx* (6). A key component of our current project is investigating the therapeutic potential of sarcospan in D2.*mdx* mice. Earlier publications identify sarcospan as an important regulator of muscle cell adhesion, strength, and regeneration (7-9). Prior research conducted on dystrophin-deficient *mdx* mice has shown that overexpression of sarcospan resulted in improved muscle stem and progenitor cell function in

cells grown on an *mdx*-derived matrix (10). As a result, D2.*mdx*^{TG} mice where sarcospan is overexpressed have been created to test whether sarcospan overexpression can ameliorate the disease pathology in this severe model of DMD.

CHAPTER 1: DETERMINE WHETHER SARCOSPAN OVEREXPRESSION INFLUENCES DYSTROPHIC MUSCLE PATHOLOGY

Introduction

We examined the possible therapeutic effects of sarcospan overexpression on several pathological attributes in D2.*mdx* mice: central nucleation, cross-sectional area (CSA), calcification of muscle tissues, collagen content, and fibrosis. Centrally located nuclei are signs of stress and have been previously linked to muscle dysfunction (11)(12). Previous research has shown that the B10.*mdx* mice have an increase in central nucleation due to chronic degeneration and regeneration cycles of muscle repair. Gibbs *et al*. shows that in transgenic mice, overexpression of sarcospan can reduce the number of centrally located nuclei compared to the B10.*mdx* mice (13). Overall, D2.*mdx* and B10.*mdx* mice had many more small-sized myofibers than wild-type (WT) mice, along with numerous large, hypertrophic fibers (14, 15). The difference in the cross-sectional area can be attributed again to the constant degeneration and regeneration cycles seen in *mdx* mice. Therefore, we wanted to explore whether our D2.*mdx*^{TG} mice would restore the fiber size distribution to match WT.

Intramuscular calcification is a phenotype seen only in the D2.*mdx* murine model (5). Although this phenotype is not seen in DMD patients, I was interested in examining the potential outcome that overexpressing sarcospan may have on this calcification, given its ability to restore sarcolemmal stability. Lastly, previous reports of the D2.*mdx* model suggest that this mouse line demonstrates increased skeletal muscle fibrosis (6). The increased fibrosis can be attributed in part to the latent transforming growth factor beta binding protein 4 (LTBP4) polymorphism in the D2.*mdx* mice (5). When a muscle is injured, transforming growth factor beta (TGFβ) is activated and triggers downstream SMAD signaling to repair and restore the muscle. In the murine model of D2.*mdx* dystrophic muscle, elevated TGFβ activity is observed due to a polymorphism in the LTBP4 gene, which worsens the inflammatory response and

aggravates the fibrotic response (16). The fibrosis is consistent with increased collagen production. As a result, we wanted to investigate whether sarcospan would reduce the amount of collagen - a proxy for reduced fibrosis.

Material and Methods

Animals

This study used D2.*mdx* (IMSR_JAX:013141) and D2.WT (IMSR_JAX:000671) mice, which are on the DBA/2J background with and without a genetic mutation in the dystrophin gene from Jackson Laboratories. These mice were crossbred with C57Bl/10 mice overexpressing the human sarcospan gene (C57Bl/10:hSSPN-Tg). The F1 generation was back-crossed for six generations to obtain the desired genotype. (D2.*mdx*^{TG}). Mice were maintained in the Terasaki Life Sciences Vivarium following guidelines established by the Institutional Animal Care and Use Committee at the University of California, Los Angeles (approval #2000-029- 43). Male and female mice were used for this specific aim. Mice ranged from 14-20 weeks of age.

Histological Stains

Muscles were loaded into cassettes and flash-frozen in liquid nitrogen and stored at -80 ℃. Once needed, the muscles were coated in OCT in preparation for sectioning. Transverse 15μm sections were stained with Hematoxylin and Eosin (H&E), Alizarin Red (Sigma-Aldrich #TMS-008-C), or Picrosirius Red (Statlab #KTPSRPT). H&E stain was used to visualize and quantify central nucleation and muscle fiber size in the quadricep and gastrocnemius muscles, as previously described (29). Alizarin Red stain was used to visualize and quantify intramuscular calcification in quadricep and diaphragm tissues. Picrosirius Red stain was used to visualize collagen in the gastrocnemius muscle. Alizarin Red and Picrosirius Red staining procedures were performed in accordance with the manufacturers' directions.

Image Quantification and Statistical Analysis

ImageJ software was used to quantify all histological stains. For the Picrosirius Red stain, I used the “Colour Deconvolution” plugin for ImageJ to calculate the percentage of collagen in each examined tissue. Prism 10 software was used to run a nested analysis of all the data obtained. One-way ANOVA followed by Tukey’s multiple comparisons tests were used to calculate statistical significance (*P < 0.05, **P < 0.01, ***P < 0.001 and ****P <0.0001).

Results

In our study of the connection between SSPN overexpression, myofiber structure, and histopathology, we noted several restorative changes in the D2.*mdx*^{TG} mice. To analyze the characteristics of skeletal muscle fibers, we used histological staining with hematoxylin and eosin (H&E) on transverse sections of the skeletal muscle. The D2.*mdx*^{TG} mice muscle sections revealed similar histopathological features to those of the D2.WT mice. Upon analyzing the H&E stains, we observed an overall decrease in the amount of centrally located nuclei (CLN) in both quadriceps and gastrocnemius tissue for our D2.*mdx*^{TG} mice (Fig. 1.1-1.2). However, elevated levels of centrally located nuclei remained in the D2.*mdx*^{TG} mice in comparison to the D2.WT. This difference is due to the a high density of CLNs in small pockets of muscle fibers in D2.*mdx*^{TG} mice, while the majority of the section has little to no CLN presence – indicating there is still myofibril damage in our transgenic model.

In an attempt to discern the therapeutic potential of the D2.*mdx*^{TG} mice, we examined the cross-sectional areas of each muscle fiber. As previously mentioned, an increased prevalence of smaller muscle fibers is an indication of muscle degeneration and regeneration. For the cross-sectional area of D2.WT mice, the average CSA was approximately 2000 μm^2. The average CSA fiber size in D2.*mdx* mice was under 1000 μm^2. In some instances, there were myofibers around 10,000 μm^2, representing hypertrophic fibers. This heterogeneity was more evident in the D2.*mdx* mice than D2.WT and D2.*mdx*^{TG}. Overall, the median fiber size of the D2.*mdx*^{TG} was partially restored to approximately 1600 μm^2. The decreased heterogeneity of

the cross-sectional area in the D2.*mdx*^{TG} mice, along with fewer small fibers, trends toward the CSA of those in wild-type mice (Fig. 1.3). The D2.*mdx*^{TG} mice reveal similar histopathology to D2.WT, as evidenced by the results of both central nucleation and cross-sectional area analysis.

It has been observed that muscle calcification, is only seen in D2.*mdx* mice and falls outside of human disease pathology (5). In the quadricep tissue, on average,D2.WT mice had less than 1% of the tissue area that showed intramuscular calcification. Analysis of D2.*mdx*^{TG} and D2.*mdx* mice showed an average calcification percentage of 6% and 3%, respectively (Fig. 1.4). This result was also observed in the diaphragm of the D2.*mdx*^{TG} mice. D2.WT mice had no intramuscular calcification in their tissue. D2.*mdx*^{TG} mice showed an increased intramuscular calcification of roughly 19% compared to 15% in the D2.*mdx* mice. (Fig 1.5).

Published literature highlights that increased fibrosis is linked to increased collagen content in dystrophic muscle. On average, D2.WT muscle contained roughly 13% collagen content in analyzed muscle sections. We noted a similar collagen percentage in gastrocnemius tissue when comparing the D2.*mdx*^{TG} mice to the D2.*mdx* using a Picrosirius Red stain to visualize collagen (Fig 1.6). The average percent of collagen content in muscle sections for D2.*mdx* and the D2.*mdx*^{TG} were 29% and 27%, respectively. This result sparked our curiosity and inspired us to investigate potential proteomic differences.

Discussion

These histological stains revealed distinct characteristics in the D2.*mdx*^{TG} mice. We noted a decrease in the amount of centrally located nuclei in D2.*mdx*^{TG} mice. As mentioned previously, increased central nucleation is the result of repeated muscle degeneration and regeneration. The decrease in centrally located nuclei supports the therapeutic potential of sarcospan overexpression - that sarcospan protects myofiber stability, which reduces the amount of regeneration that needs to take place. Small muscle fibers indicate that the fiber has

undergone regeneration, resulting in a heterogenous muscle fiber size when analyzing cross sections. D2.*mdx*^{TG} muscles had fewer small muscle fibers than the D2.*mdx*. Also, the distribution of the muscle fiber cross-sectional area mimics the distribution seen in D2.WT mice, meaning that the D2.*mdx*^{TG} mice had more homogenous fibers. This further supports the restorative effect of sarcospan overexpression in the D2.*mdx* murine model. Next, we examined the intramuscular calcification of muscle cross-sections. As mentioned previously, the D2.*mdx* mouse model has intramuscular calcification that is not noted in the human pathophysiology in DMD patients. Using Alizarin Red stains, we observed an increase in the amount of calcification in the D2.*mdx*^{TG} mice. While the potential link between SSPN and intramuscular calcification is unknown, we aimed to examine all relevant characteristics of the D2.*mdx* mouse model.

Fibrosis has been linked to increased pathology seen in mice, and skeletal muscle fibrosis typically precedes the disease pathology. The repeated contraction of the skeletal muscle resulting in micro-tears leads to an accumulation of scar tissue rich in fibrotic collagen. This fibrotic tissue makes the muscle more susceptible to future tears, and incomplete repair. When examining our therapeutic mouse model, we expected a reduction in the amount of collagen in the D2.*mdx*^{TG} mice. Using the Picrosirius Red stain and ImageJ, we did not see a reduction in the amount of collagen present in the D2.*mdx*^{TG} compared to D2.*mdx* mice. However, Stearns-Reider *et al*. showed an increase of collagen production in B10.*mdx*^{TG} mice that was independent of pathology, meaning that in the WT mice where sarcospan was overexpressed, there was noted an increase in collagen content. The increase in collagen production was indicative of a compensatory upregulation of collagen to stabilize the muscle membrane, which may confer the beneficial effects of SSPN overexpression.

CHAPTER 2: DEDUCE THE IMPACT OF SARCOSPAN OVEREXPRESSION ON MEMBRANE STABILITY

Introduction

Dystrophic muscle is characterized by repeated tears in the muscle membrane that render the membrane unstable. Specific transmembrane proteins comprise adhesion complexes that localize to the sarcolemma of the muscle cell in order to stabilize the membrane. In addition to the dystrophin-glycoprotein complex (DGC), two other major adhesion complexes are found at the sarcolemma, which is the utrophin-glycoprotein complex (UGC) and the α7β1 integrin complex (17) (18) (19). Utrophin of the UGC in WT (non-dystrophic) tissue is normally found in the neuromuscular junction (NMJ) of the muscle cell (20). The α7β1 integrin complex supports the linkage of the cytoskeleton to the ECM (19). Over time, the repeated contraction-induced damage to the membrane leads to a progressive decrease in the integrity of the membrane. Ultimately, the muscle is unable to undergo further regeneration, resulting in muscle death - necrosis. Previous work from our lab by Gibbs *et al*. overexpressed sarcospan in the B10.*mdx* mice. Through immunohistochemical analysis, they noted an increase in the amount of known proteins associated with major adhesion complexes in B10.*mdx*^{TG} mice. This finding supports the therapeutic potential of sarcospan as it can stabilize the muscle membrane by increasing the localization of adhesion complex proteins to the sarcolemma. In order to further test the physiological benefits of overexpressing sarcospan, Gibbs *et al*. noted increased peak grip strength and ambulation of transgenic mice compared to B10.*mdx.*

An increased blood serum creatine kinase (CK) is a hallmark indicator of muscular dystrophy. CK levels in DMD patients are typically elevated 50- to 200-fold above normal levels (21). Creatine kinase is an enzyme found in all types of muscle, including skeletal, and is released into the blood during muscle injury (1). This increase is due, in part, to an unstable

membrane caused by repeated muscle contractions resulting in tears. These tears in the membrane render the membrane “leaky,” resulting in an increased CK release into the serum (22). As a result, I will be examining the presence of adhesion complex proteins at the sarcolemma using immunohistochemistry. I used grip strength and open-field (ambulation) test as a proxy to measure muscle strength. Lastly, I measured serum creatine kinase levels of euthanized mice as a proxy to examine membrane leakiness.

Material and Methods

Animals

This study used D2.*mdx* (IMSR_JAX:013141) and D2.WT (IMSR_JAX:000671) mice, which are on the DBA/2J background with and without a genetic mutation in the dystrophin gene from Jackson Laboratories. These mice were crossbred with C57Bl/10 mice overexpressing the human sarcospan gene (C57Bl/10:hSSPN-Tg). The F1 generation was back-crossed for six generations to obtain the desired genotype. (D2.*mdx*^{TG}). Mice were maintained in the Terasaki Life Sciences Vivarium following guidelines established by the Institutional Animal Care and Use Committee at the University of California, Los Angeles (approval #2000-029- 43). Male and female mice were used for this specific aim. Mice ranged from 14-20 weeks of age.

Grip Strength Test

Forelimb grip strength was measured using a digital force gauge. The mouse grasped the pull bar connected to the digital gauge and was pulled back until the mouse released the pull bar. The pull was repeated five times, and the peak force generated was noted as one trial. The peak ten tensions (N) were recorded from ten trials, with 30 seconds rest between each trial. The force generated was normalized to the body weight of each mouse.

Open Field Test

An ambulation test was performed, immediately following the grip strength test. Mice were placed in individual recording chambers and allowed to freely explore for 6 minutes, which is

analogous to the 6-minute walking test post-exercise for DMD patients. Kinovea open-source video analysis was used to track the distance traveled by the mice using frame-by-frame object tracking.

Serum Creatine Kinase Test

Blood was collected while euthanizing the mice (terminal blood draw). The blood was then centrifuged to isolate and collect the serum. The serum was stored at -80℃. Total serum creatine kinase was measured using Creatine Kinase-SL Assay (Sekure Chemistry; 326-10) according to the manufacturer's instructions.

Results

With improvements we noted in the histopathology of the D2.*mdx*^{TG} mice, we wanted to explore the potential of improved muscle performance. A previous publication from our lab showed that increased sarcospan in the B10.*mdx* mice improved muscle function (13). Consequently, we wanted to see if sarcospan overexpression would also improve muscle function in the more severe murine model of DMD. The first experiment we conducted was the grip strength test. Upon analyzing the data, we did not observe an improved grip strength in D2.*mdx*^{TG} mice compared to D2.*mdx* (Fig. 2.1). Of the 10 trials that were conducted, there were multiple trials where D2.*mdx*^{TG} generated less force than the D2.*mdx* mice. Following the completion of the grip strength test, we transitioned in the open-field test. Similarly, we did not observe a recovery of voluntary movement in the ambulation test (Fig. 2.1). D2.*mdx*^{TG} on average travelled shorter distances than the D2.WT and D2.*mdx*. As the trial progressed, there was no improvement in the performance of the mice. For both strength tests, D2.*mdx*^{TG} mice exhibited a significant decline in muscle strength.

We wanted to investigate the integrity of the muscle membrane next. Creatine kinase presence in the blood serum is a well-known marker of muscle damage (1). As expected,

D2.*mdx* mice had increased serum creatine kinase levels compared to D2.*mdx*. Our results show a restoration of serum creatine kinase levels in D2.*mdx*^{TG} mice, similar to the levels seen in D2.WT. (Fig. 2.2).

Discussion

The current results show a disconnect form membrane stability and muscle function. Grip strength for the D2.*mdx*^{TG} mice was not restored compared to the D2.*mdx* mice. Ambulation data did not show a recovery of voluntary movement for D2.*mdx*^{TG} mice. This does not support the original hypothesis. We will use proteomic analysis to examine whether SSPN overexpression alters these adhesion complex proteins, which will provide evidence that this is a localization issue.

Lastly, we analyzed the serum creatine kinase levels of the terminal blood draws for these mice and noted a decrease in the amount of creatine kinase found in the serum of D2.*mdx*^{TG} mice similar to levels in D2.WT mice. These results suggest that improved muscle repair occurs in the D2.*mdx*^{TG} mice in comparison to the D2.*mdx*. Also, it suggests the mouse muscle membranes are less “leaky” and more stable.

Although there wasn’t an improvement in the muscle strength of our D2.*mdx*^{TG} mice, we did note an improvement in the stability of the sarcolemma. It is important to note that D2.*mdx* mice show improvement in disease pathology as they age (14), which is contrary to what is observed in the B10.*mdx* murine model. We are in the process of aging mice to examine whether sarcospan overexpression is able to recover muscle function. Nevertheless, these results are promising as they show that sarcospan is able to improve the overall architecture of the muscle, which is a vital step forward to discovering a therapeutic for DMD.

CHAPTER 3: ANALYZE PROTEOMIC DATA ON THE IMPACT OF SARCOSPAN OVEREXPRESSION

Introduction

In order to examine the therapeutic effects of overexpressing sarcospan and to identify proteins and pathways responsible for changes seen in the D2.*mdx*^{TG} mice, we used proteomic data. We are working with Dr. Hansen at the University of Colorado to get quantitative proteomic data on the matrisome of the D2 mouse quadriceps, along with global qualitative proteomics. Gibbs *et al*. presented data showing an increase in the amount of adhesion complex proteins in the muscles of transgenic mice compared to the B10.*mdx.* Global proteomic data obtained from our D2.*mdx* mice allow us to provide more evidence supporting sarcospan's role in increasing the production of proteins known to stabilize the sarcolemma.

As previously mentioned, there is an increase in the amount of collagen between the D2.WT compared to the D2.*mdx and* D2.*mdx*^{TG} mice. Although an increase in collagen production has been linked to an increase in fibrosis, a previous study from our lab shed light on a possible new role of collagen in D2.*mdx*^{TG} mice, a form of compensatory regulation. Stearns-Reider *et al*. examined the role of the ECM and how scarring (due to fibrosis) affects skeletal muscle progenitor cell (SMPC) activation in the B10.*mdx* mice. One of the conclusions she made was that laminin, not collagen, was responsible for reduced SMPC function. In fact, increased collagen in transgenic B10.*mdx* mice supported robust SMPC function. She also examined transgenic B10.WT mice and noted increased collagen content. As a result, she concluded that the increased collagen deposition was independent of the dystrophic pathology. To elucidate the role of SSPN in collagen abundance, we decided to harvest the power of quantitative proteomics to examine changes in the relative and absolute abundance of major collagen proteins in the D2.*mdx*^{TG} mice compared to the D2.*mdx*. QconCAT quantification is a new method of quantifying desired proteins. QconCAT analysis uses a known quantity of

concatenated peptides to quantify peptides that can be reproducibly generated from a sample, quadriceps muscle in our case (23). This quantification method allows us to obtain absolute quantities of proteins, and investigate their relative contributions to the matrisome as a whole. The relative abundance reflects the stoichiometry of the proteins, while the absolute abundance is the total amount of protein present.

Fibrillar collagens play a role in providing three-dimensional frameworks for tissues and organs by creating networks to provide mechanical strength as well as signaling to components of the ECM (24). FACIT collagens anchor the sarcolemma to the ECM by binding to the fibrillar collagens (25). Both Fibrillar and FACIT collagens work in unison to uphold the integrity of the ECM. Although these collagens have similar roles in sustaining the integrity of the ECM, the composition of these proteins can be altered depending on the dystrophic state. As a result, we also examined the solubility of these proteins. Protein solubility is important when considering whether the collagens are contributing to a fibrotic environment. Insoluble collagens are linked to contributing to a stiffer and, as a result, fibrotic membrane. We examined the solubility index, a measure of the percentage of soluble versus total protein content, of the D2.WT mice and compared solubility to the D2.*mdx* and D2.*mdx*^{TG} mice. Lastly, we went further and examined the solubility of individual major collagen proteins such as Col1A1, Col1A2, Col3A1, Col5A1, and Col5A2.

Materials and Methods

Animals

This study used D2.*mdx* (IMSR_JAX:013141) and D2.WT (IMSR_JAX:000671) mice, which are on the DBA/2J background with and without a genetic mutation in the dystrophin gene from Jackson Laboratories. These mice were crossbred with C57Bl/10 mice overexpressing the human sarcospan gene (C57Bl/10:hSSPN-Tg). The F1 generation was back-crossed for six

generations to obtain the desired genotype. (D2.*mdx*^{TG}). Mice were maintained in the Terasaki Life Sciences Vivarium following guidelines established by the Institutional Animal Care and Use Committee at the University of California, Los Angeles (approval #2000-029- 43). Male and female mice were used for this specific aim. Mice ranged from 14-20 weeks of age.

Proteomic Analysis

Flash-frozen mice quadricep tissue was shipped to Dr. Hansen at the University of Colorado to get quantitative proteomic data on the matrisome of these D2 mouse quads. The Hansen lab uses a digestion method that allows the cellular, soluble, and insoluble fractions to be run independently, providing a comprehensive analysis of the matrix proteins present in the samples. The optimized three-step decellularization and ECM extraction method involved chaotropic extraction and digestion via hydroxylamine hydrochloride as previously described (30). There were a total of 5 wild-type, 9 D2.*mdx*, 5 D2.*mdx*^{TG} mice.

Results

As previously mentioned, there is a polymorphism of the LTBP4 gene that results an increase in TGFb1 activation. This polymorphism is responsible for the phenotype we examine in the D2.*mdx* model (5). Total protein content for D2.*mdx* mice showed increased levels of TGFb1 (Fig. 3.1A). Next, we confirmed our mouse model and the DMD murine models by analyzing the total protein levels of sarcospan and dystrophin. As expected, D2.*mdx*^{TG} mice had increased sarcospan protein content (Fig. 3.1B). D2.*mdx* and D2.*mdx*^{TG} mice both had relatively no dystrophin protein levels (Fig 3.1C). The global proteomics for the mice quadriceps shows an increase or restoration in the total abundance of sarcolemma-supporting proteins such as sarcoglycans, utrophin, and dystroglycans in D2.*mdx*^{TG} mice. a-Sarcoglycan and g-Sarcoglycan protein levels were increased in D2.*mdx*^{TG} mice in comparison to D2.WT and D2.*mdx* protein content, while b-Sarcoglycan and d-Sarcoglycan protein levels in the D2.*mdx*^{TG} was restored to D2.WT levels. (Fig. 3.1D-J). Next, quantitative proteomic analysis of the fibrillar collagen

ratios showed there was no difference between the three genotypes (Fig. 3.2). Although the distribution of the fibrillar collagen remained unchanged, the total abundance was altered. The amount of fibrillar collagen did increase in both D2.*mdx* and D2.*mdx*^{TG} mice in comparison to D2.WT mice (Fig. 3.2). This result was similar for FACIT collagen distribution (Fig. 3.2). The total amount of FACIT collagens was also increased in both D2.*mdx* and D2.*mdx*^{TG} mice (Fig. 3.2).

Next, we examined the solubility of collagen proteins. There was an increase in the amount of soluble fibrillar collagen in D2.*mdx*^{TG} mice, similar to WT solubility (Fig. 3.3). This again supports the idea of a less fibrotic collagen composition in the D2.*mdx*^{TG} mice. The solubility of FACIT collagens was similar for all three genotypes (Fig. 3.3). Afterward, we examined major collagen proteins and noted restoration of soluble collagen in Col3a1, Col5a1, and Col5a2 proteins {Fig 3.4}. Lastly, we examined global proteomic data on a known cross-linking enzyme, Lox. The total amount of Lox enzyme was decreased in D2.*mdx*^{TG} mice, similar to D2.WT levels (Fig. 3.5).

Discussion

While addressing the connection between SSPN overexpression and its therapeutic ability to ameliorate dystrophic histopathology and subsequent muscle degeneration, we wanted to observe the potential changes that were occurring on a proteomic level. Upon analyzing the total protein content of adhesion complex proteins, we found that sarcoglycan protein levels were either compensatory increased in or returned to D2.WT levels. The total protein content of utrophin was also increased in D2.*mdx*^{TG} mice in comparison to D2.WT and D2.*mdx*. Prior publications support the idea that utrophin upregulation assists in aiding dystrophic muscle with the absence of dystrophin in the B10.*mdx* murine model (26). Lastly, dystroglycan protein levels were also upregulated in D2.*mdx*^{TG} mice in comparison to both D2.WT and D2.*mdx* protein content. This result reaffirms sarcospan's role in upregulating these proteins that were seen in

previous publications from our lab (13). Although the total protein production was increased, more work is needed to determine how these proteins influence disease progression.

Previous publications show the compensatory role of collagen in stabilizing the dystrophic membrane and activating SMPCs (10). QConCAT data of fibrillar and FACIT collagens show changes in both D2.*mdx* and D2.*mdx*^{TG} mice. Although the relative abundance of these collagen proteins was not altered between the three genotypes, the total amount of protein was increased in both D2.*mdx* and D2.*mdx*^{TG} mice for both fibrillar and FACIT collagens. The difference between the two collagens families was the solubility of the proteins. Upon analyzing the solubility index of the two classes of collagen, D2.*mdx*^{TG} mice had increased solubility of fibrillar collagen than D2.*mdx*. This decrease in the amount of insoluble collagen indicates there is less fibrotic “stiff” collagen in D2.*mdx*^{TG} mice. Fibrosis will render the membrane less fluid, which in turn would decrease the natural flexibility of the membrane during muscle contractions. Next, we analyzed major fibrillar collagen proteins such as Col1a, Col3a, and Col5a, along with their respective subtypes. Col3a1 and Col5a1-2 had an increase in soluble collagen relative to D2.*mdx* mice, again showing restoration of collagen solubility to near D2.WT levels.

Lastly, with the abundance of data from the proteomic analysis, we compared the amount of Lox protein in D2.*mdx* and D2.*mdx*^{TG} mice. The Lox protein is a known cross-linking enzyme that is linked to collagen fibrosis. Lox protein expression was decreased in D2.*mdx*^{TG} mice in comparison to D2.*mdx*. We cannot conclusively determine if there is less cross-linking in D2.*mdx*^{TG} mice without a co-stain to visualize and quantify the cross-linking in muscle sections. Nevertheless, our working hypothesis is that the decrease in cross-linking in D2.*mdx*^{TG} mice contributes to the differences between D2.*mdx* and D2.*mdx*^{TG} mice.

CONCLUSION

This study aimed to discover the therapeutic potential of sarcospan overexpression in a more severe model mouse model of DMD. We observed a decrease in histopathology in the D2.*mdx*^{TG} mice with the reduction of central nucleation in muscle sections and restoration of cross-section area distribution similar to WT levels. Surprisingly, intramuscular calcification was increased in the D2.*mdx*^{TG} mice. Intramuscular calcification is only seen in the D2.*mdx* murine model for DMD but is not observed in human disease. Nonetheless, this result raises questions on whether sarcospan has off-target effects of upregulated other molecular pathways that involve calcium, possibly bone-related pathways. Another surprising outcome of our histopathological analysis of the therapeutic effect of sarcospan overexpression was the similar amount of collagen content in D2.*mdx*^{TG} mice relative to D2.*mdx*. Although collagen is linked to fibrosis, I was interested in investigating the changes in collagen content at a protein level, which prompted the use of quantitative proteomics.

The results from our experiments to test membrane stability and muscle strength for the D2.*mdx*^{TG} mice showed no significant improvement. The grip strength and open-field test results were surprising, given the fact we noted improvement in overall muscle pathology. These results may be attributed to the age of the mice that were used in the experiment. As previously mentioned, D2.*mdx* recovery is more effective as the mice age, which is unorthodox from standard muscle disease progression. We are currently in the process of aging mice and reinitiating these muscle strength tests to see if sarcospan aids in the recovery of D2.*mdx* mice. Serum creatine kinase levels were reduced in the D2.*mdx*^{TG} mice, which indicated less muscle damage and improved muscle cell membrane stability.

Quantitative proteomic data indicates an increase in adhesion complex proteins known to stabilize the muscle membrane and provide mechanical stability that is necessary for muscle

function in D2.*mdx*^{TG} mice. This affirms previous publications that sarcospan overexpression is responsible for the upregulation of these sarcolemma-supporting proteins. Shifting our focus to investigating collagen's role in the D2.*mdx* mouse model, we noted an increase in the absolute abundance of fibrillar and FACT collagens in both D2.*mdx* and D2.*mdx*^{TG} mice. The relative abundance (ratios) of these collagens was unchanged. The one area of difference was the solubility of these collagen proteins. Fibrillar collagen in the D2.*mdx*^{TG} mice had an increased solubility index for total fibrillar collagen and major collagen proteins such as Col3a1, Col5a1, and Col5a2. This substantiates the hypothesis that collagen may have a compensatory and emerging role in stabilizing the muscle membrane in D2.*mdx*^{TG} mice. Lastly, Lox protein expression was decreased in the D2.*mdx*^{TG} mice, similar to WT levels. Cross-linking of collagen in the matrix results in a stiffer, non-ideal environment for muscle regeneration. The decrease in Lox protein expression is likely a contributing factor for seeing differences in cross-linking between D2.*mdx* and D2.*mdx*^{TG} mice, which would create a more favorable environment for muscle regeneration.

Our study was able to investigate the D2.*mdx* murine model successfully and the role of sarcospan as a therapeutic for DMD. The therapeutic potential of sarcospan is promising based on the results of this study. It also opens avenues for future research and discussion for using the D2.*mdx* model as the gold standard for DMD research. Future directions include investigating the D2.*mdx*^{TG} mice at varying ages, as the D2 murine model has shown improvement in muscle pathology as it ages.

It is important to note that this paper does not include immunohistological stains of sarcospan-supporting proteins such as Utrophin, Integrin, Sarcoglycans, and their respective subunits. We are in the process of investigating the unique pathology in the D2.*mdx* mouse line that is presenting technical challenges when interpreting results as having biological significance. One challenge to note is the relative “stickiness” of the D2.*mdx* membrane, which results in clumping of immunohistological primary proteins and binding of those proteins to the

extracellular components of the muscle myofibril rather than the sarcolemma. To combat this issue, we are in the process of using TrueBlack IF background suppressor to increase our efforts to obtain clean, biologically relevant data. Lastly, the possible restructuring of the muscle membrane in the D2.*mdx* mouse model is worth investigating. This can be accomplished by using co-stains such as Laminin-2 and Collagen-1, which allow one to view the architecture of the muscle membrane.

Our current findings provide insight in the therapeutic potential of SSPN overexpression in the D2.*mdx* murine model. This study provides histopathological, physical (muscle function), and proteomic analysis of the more severe murine model of DMD. We noted an improvement in histological pathology regarding central nucleation and myofibril cross-sectional area. Although the muscle functionality and strength were not restored in D2.*mdx*^{TG}, we noted a drastic improvement in the architecture of the sarcolemma, demonstrating restored membrane stability in D2.*mdx*^{TG} mice. This is a critical first step to improve muscle function in dystrophic mice.

The similarity of the collagen content between our D2.*mdx*^{TG} and D2.*mdx* paved a new road to investigate the potential difference in the proteomic changes in collagen content between these two mice lines. The employment of quantitative and global proteomics provided relative and absolute protein contents in the matrisome, allowing us to view changes in the ECM between all three genotypes. Although the total content of the collagen remains the same between D2.*mdx*^{TG} and D2.*mdx* mice, there is a compensatory upregulation of fibrillar collagens in our transgenic murine model. The solubility of fibrillar collagen also changed towards the same levels of D2.WT indicates a less stiff matrix suitable for muscle regeneration. Taken together, these findings demonstrate sarcospan's ability to create an environment that is favorable for muscle regeneration and repair.

FIGURES

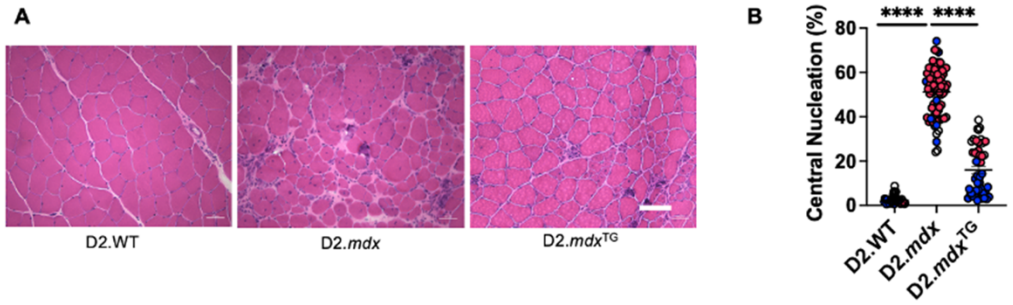

Figure 1.1: Sarcospan overexpression improves muscle histology in D2.*mdx* mice quadriceps. (**A)** Transverse sections of quadriceps muscle from 14-20 week old D2.WT, D2.*mdx*, and D2.*mdx*^{TG} were stained with Hematoxylin and Eosin (H&E) to visualize muscle pathology (D2.WT n=5, D2.*mdx* n=9, D2.*mdx*^{TG} n=5). (**B**) D2.*mdx*^{TG} quadriceps display reduced central nucleation relative to D2.*mdx*. The different colors for each genotype represent data from different mice. Bar, 50μm. Statistics were calculated using one-way ANOVA followed by Tukey's multiple comparison's test (*P < 0.05, **P < 0.01, ***P < 0.001 and ****P <0.0001).

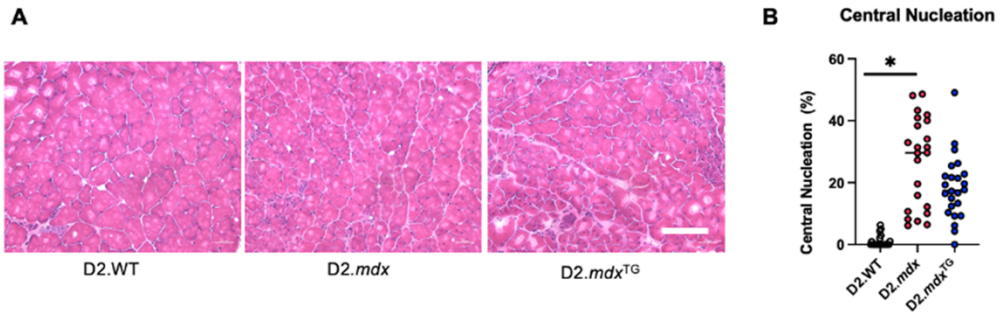

Figure 1.2: Sarcospan overexpression improves muscle histology in D2.*mdx* mice gastrocnemius. (**A)** Transverse sections of quadriceps muscle from 14-20 week old D2.WT, D2.*mdx*, and D2.*mdx*^{TG} were stained with Hematoxylin and Eosin (H&E) to visualize muscle pathology (D2.WT n=3, D2.*mdx* n=3, D2.*mdx*^{TG} n=3). (**B**) D2.*mdx*^{TG} gastrocnemius display reduced central nucleation relative to D2.*mdx*. Bar, 50μm. Statistics were calculated using one-way ANOVA followed by Tukey's multiple comparison's test (*P < 0.05, **P < 0.01, ***P < 0.001 and ****P <0.0001).

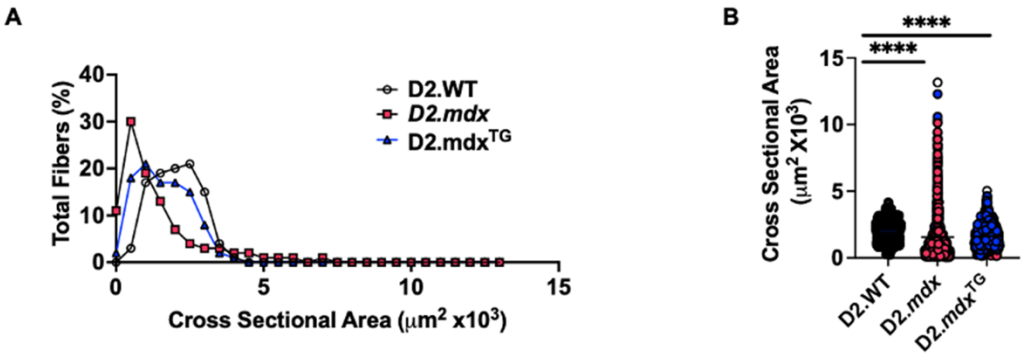

Figure 1.3: Restoration of muscle fiber cross-section area (CSA) in sarcospan overexpressed mice. (**A**) Fiber-size frequency distribution was assessed for quadricep muscles for 14-20 week old D2.WT, D2.*mdx*, and D2.*mdx*^{TG} mice muscle sections were stained with hematoxylin and eosin (H&E). Findings suggest restoration of fiber size distribution of muscle sections similar to wild-type. (**B**) The total cross-section area was calculated. Statistics were calculated using one-way ANOVA followed by Tukey's multiple comparison's test (*P < 0.05, **P < 0.01, ***P < 0.001 and ****P <0.0001).

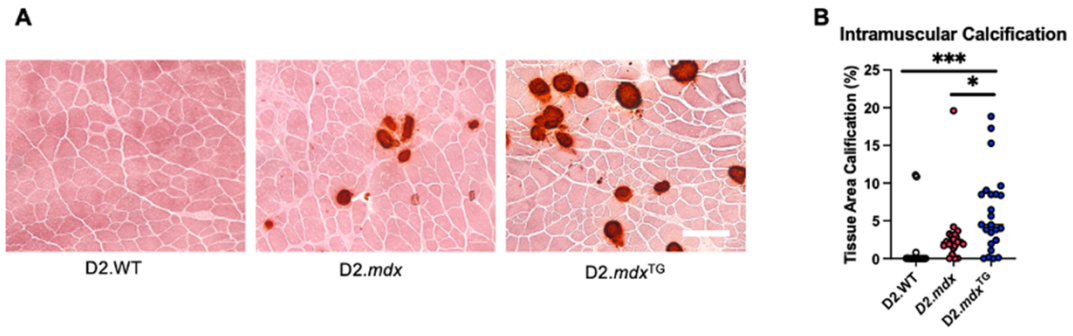

Figure 1.4: Increased Intramuscular calcification in quadricep muscle of D2.*mdx*^{TG} mice. (**A**) Transverse sections of quadriceps muscle from 14-20 week old D2.WT, D2.*mdx*, and D2.*mdx*^{TG} were stained with Alizarin Red to visualize intramuscular calcification (D2.WT n=3, D2.*mdx* n=3, D2.*mdx*^{TG} n=3). (**B**) D2.*mdx*^{TG} quadriceps display increased intramuscular calcification relative to D2.*mdx*. Bar, 50μm. Statistics were calculated using one-way ANOVA followed by Tukey's multiple comparison's test (*P < 0.05, **P < 0.01, ***P < 0.001 and ****P <0.0001).

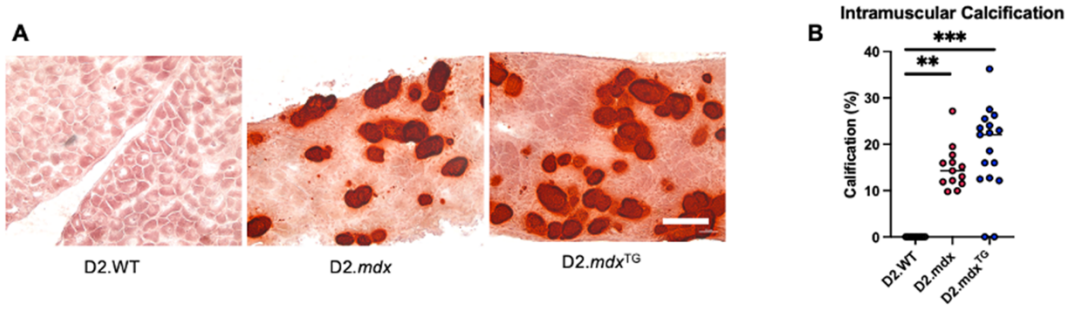

Figure 1.5: Alizarin Red stain shows the prevalence of calcification of tissue in D2.*mdx*^{TG} mice diaphragms. (**A**) Transverse sections of diaphragm muscle from 14-20 week-old D2.WT, D2.*mdx*, and D2.*mdx*^{TG} were stained with Alizarin Red to visualize intramuscular calcification (D2.WT n=3, D2.*mdx* n=3, D2.*mdx*^{TG} n=3). (**B**) D2.*mdx*^{TG} diaphragm display increased intramuscular calcification relative to D2.*mdx*. Bar, 50μm. Statistics were calculated using one-way ANOVA followed by Tukey's multiple comparison's test (*P < 0.05, **P < 0.01, ***P < 0.001 and ****P <0.0001).

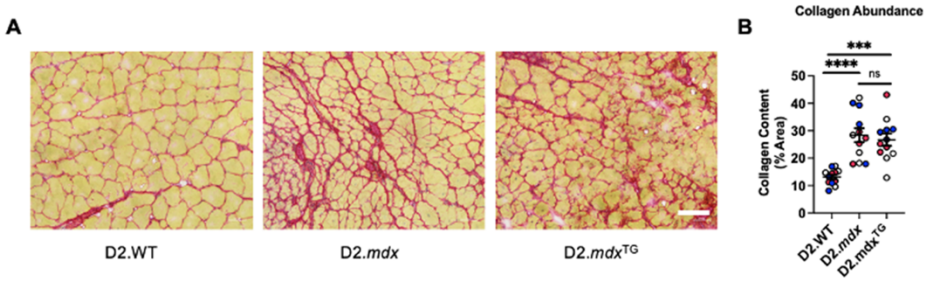

Figure 1.6: Sarcospan overexpressed mice showed similar collagen content to D2.*mdx* mice. (**A**) Transverse sections of gastrocnemius muscle from 14-20 week-old D2.WT, D2.*mdx*, and D2.*mdx*^{TG} were stained with Picrosirius Red to visualize intramuscular calcification (D2.WT n=3, D2.*mdx* n=3, D2.*mdx*^{TG} n=3). (**B**) D2.*mdx*^{TG} gastrocnemius has similar collagen content relative to D2.*mdx* mice. Bar, 50μm. Statistics were calculated using one-way ANOVA followed by Tukey's multiple comparison's test (*P < 0.05, **P < 0.01, ***P < 0.001 and ****P <0.0001).

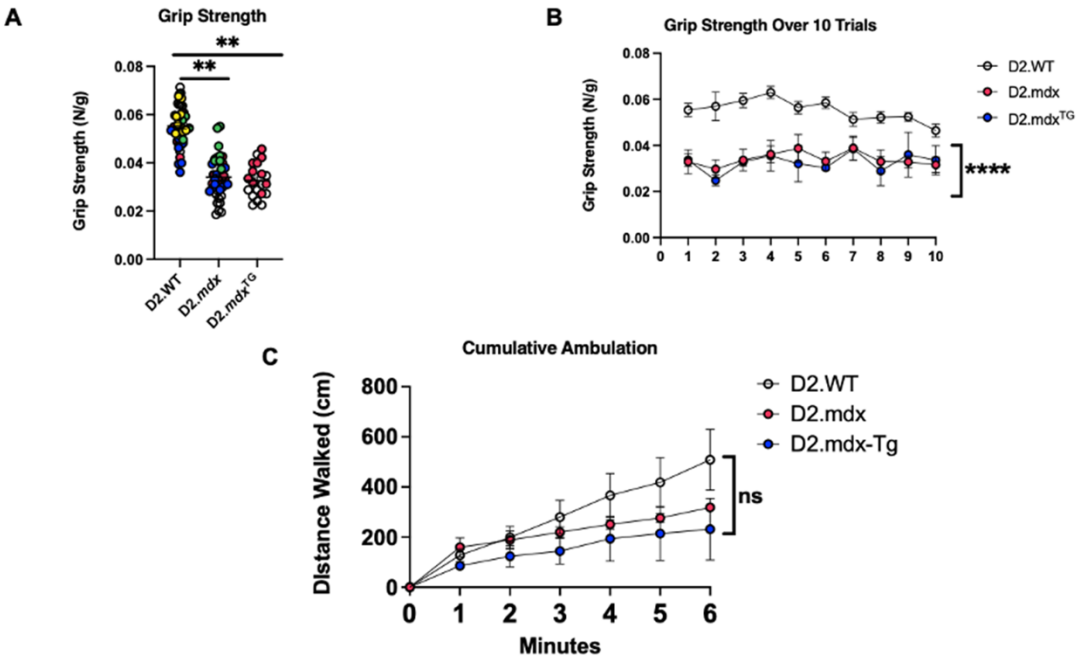

Figure 2.1: No physiological improvement of muscle strength for D2.*mdx*^{TG} mice.
(**A)** Forelimb grip strength normalized to body weight at 4-20 weeks of age (fifth consecutive trial reported). (**B)** Diagram of peak value from 10 trials of forearm grip strength. The fifth value was recorded for each individual trial. D2.*mdx*^{TG} grip strength does not recover to wild-type levels. (**C**) Post-exercise walking distances of 14-20 week-old mice were recorded using an open-field test. D2.*mdx*^{TG} mice voluntary movement is not recovered (D2.WT n=5, D2.*mdx* n=4, D2.*mdx*^{TG} n=2)

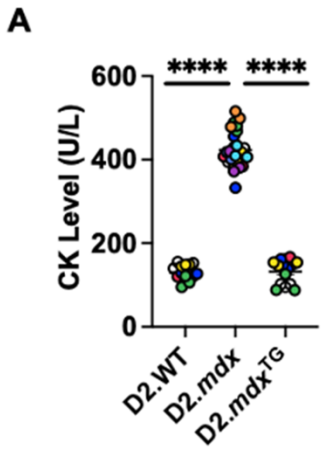

Figure 2.2: Decrease in the amount of creatine kinase in serum of D2.*mdx*^{TG} mice.
(**A**) Serum was harvested from terminal blood drawn from 14- 20 week-old D2.WT, D2.*mdx*, and D2.*mdx*^{TG} mice (D2.WT n=5, D2.*mdx* n=9, D2.*mdx*^{TG} n=5). The different colors for each genotype represent data from different mice. Statistics were calculated using one-way ANOVA followed by Tukey's multiple comparison's test (*P < 0.05, **P < 0.01, ***P < 0.001 and ****P <0.0001).

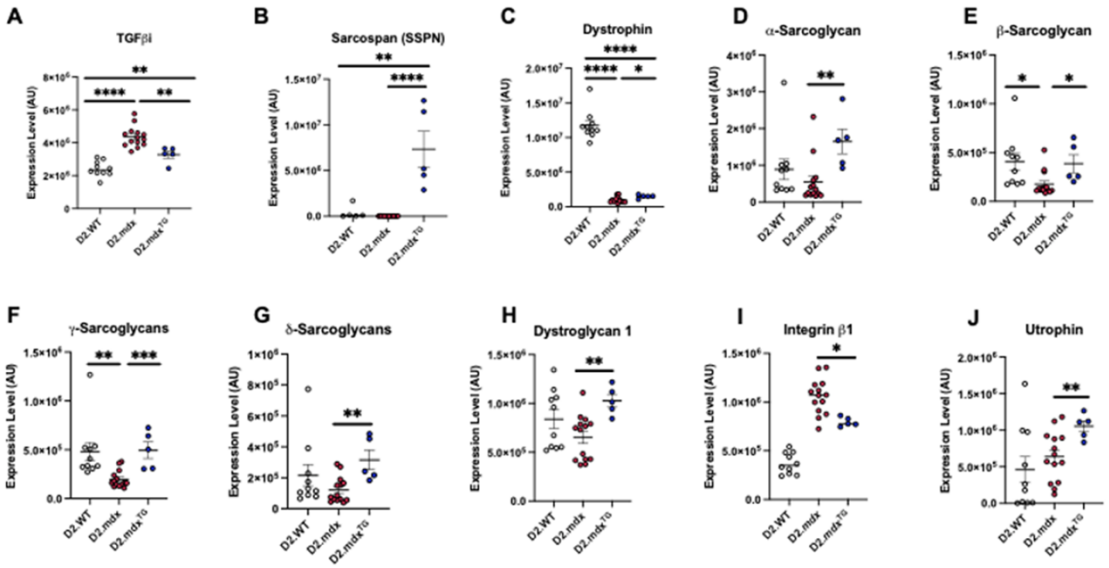

Figure 3.1: Global Proteomic analysis of major adhesion complex proteins. 14-20 week-old D2.WT, D2.*mdx*, and D2.*mdx*^{TG} quadricep muscle were analyzed using quantitative proteomics. (**A)** Global proteomic data analysis of Tumor Growth Factor beta-induced cytokine expression levels that are responsible for D2.*mdx* muscle pathology. (**B-J**) Global proteomic data analysis of major transmembrane protein expression levels is plotted above (D2.WT n = 5, D2.*mdx* n = 9, D2.*mdx*^{TG} n = 5). Statistics were calculated using one-way ANOVA followed by Tukey's multiple comparison's test (*P < 0.05, **P < 0.01, ***P < 0.001 and ****P <0.0001).

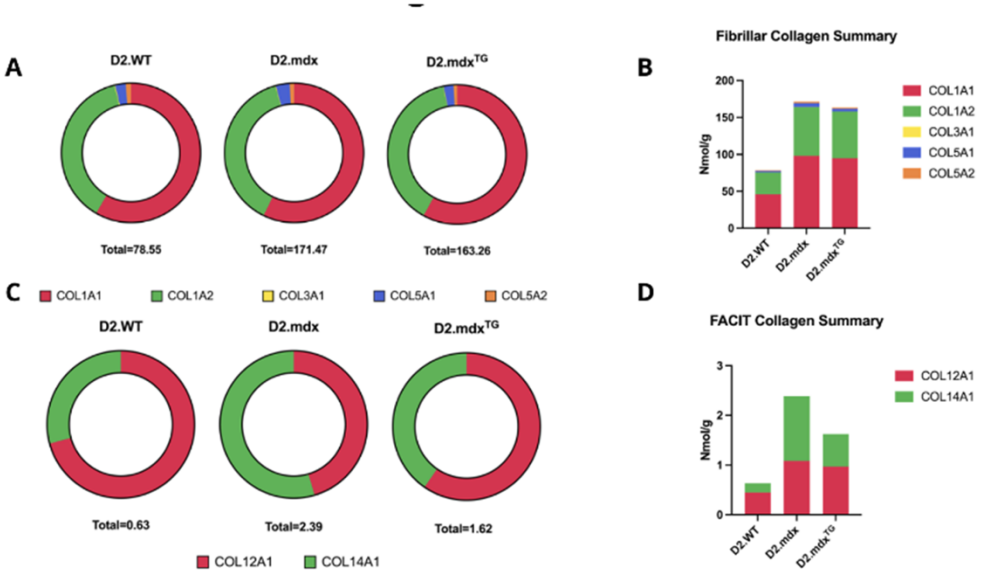

Figure 3.2: Quantitative Proteomics highlights changes in Fibrillar and FACIT collagens. (**A**) Relative abundance of fibrillar collagen proteins in the quantitative QconCAT proteomics. Pie chart shows the percentage of each protein that makes up the functional class, with the total Nmol/g listed below. (**B**) Absolute abundance of each protein in the fibrillar collagen functional class. (**C)** Relative abundance of FACIT collagen proteins in the quantitative QconCAT proteomics. Pie chart shows the percentage of each protein that makes up the functional class, with the total Nmol/g listed below. (**D)** Absolute abundance of each protein in the FACIT collagen functional class. (D2.WT n=5, D2.*mdx* n=9, D2.*mdx*^{TG} n=5).

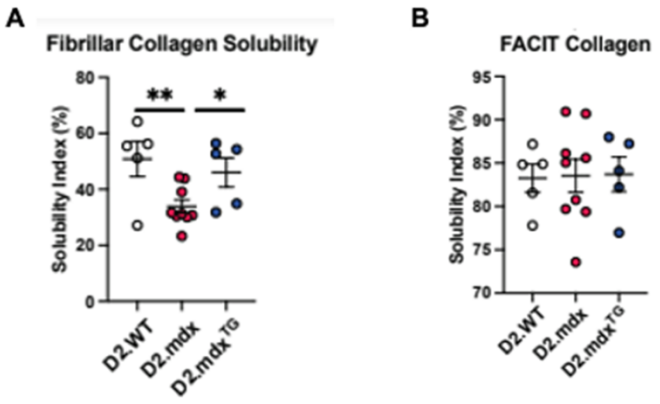

Figure 3.3: Increase in the amount of soluble collagen in D2.*mdx*^{TG} mice similar to wild-type. Examine the solubility of collagen proteins from QConCAT proteomics (D2.WT n=5, D2.*mdx* n=9, D2.*mdx*^{TG} n=5). (**A**) Restoration of soluble Fibrillar collagen to wild-type levels in D2.*mdx*^{TG} mice. (**B**) The solubility of FACIT collagens remains unchanged in comparison to D2.WT and D2.*mdx*. Statistics were calculated using one-way ANOVA followed by Tukey's multiple comparison's test (*P < 0.05, **P < 0.01, ***P < 0.001 and ****P <0.0001).

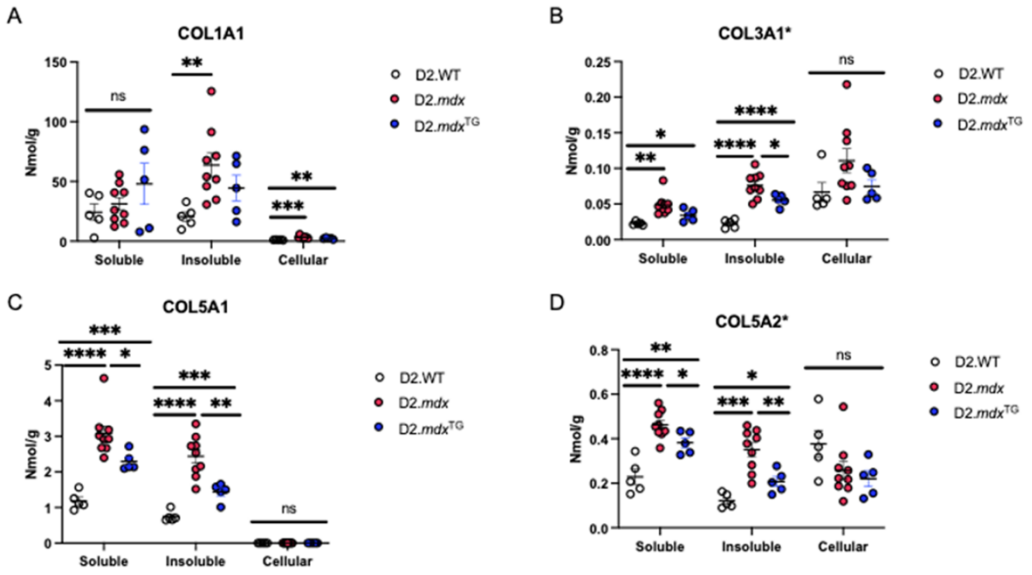

Figure 3.4: Increased soluble Fibrillar collagens in D2.*mdx*^{TG} mice. (**A-D**) Highlight major collagen proteins. There is a restoration of soluble collagen levels for the D2.*mdx*^{TG} mice (D2.WT n=5, D2.*mdx* n=9, D2.*mdx*^{TG} n=5). Statistics were calculated using one-way ANOVA followed by Tukey's multiple comparison's test (*P < 0.05, **P < 0.01, ***P < 0.001 and ****P <0.0001).

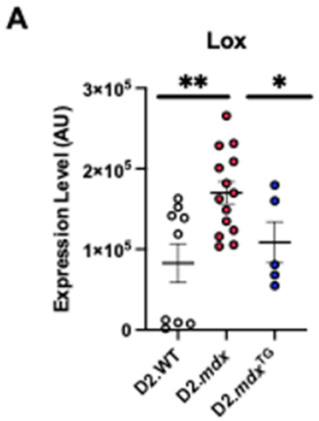

Figure 3.5: Decrease in the amount of known cross-linking enzyme in D2.*mdx*^{TG} mice. (**A**) Global proteomic data analysis of major cross-linking enzyme protein expression levels is plotted above (D2.WT n = 5, D2.*mdx* n = 9, D2.*mdx*^{TG} n = 5). There is a reduction in the amount of Lox protein in D2.*mdx*^{TG} mice. Statistics were calculated using one-way ANOVA followed by Tukey's multiple comparison's test (*P < 0.05, **P < 0.01, ***P < 0.001 and ****P <0.0001).

REFERENCES

1. Aartsma-Rus A, Ginjaar IB, Bushby K. The importance of genetic diagnosis for Duchenne muscular dystrophy. J Med Genet. 2016;53(3):145-51.

2. Emery AE. Population frequencies of inherited neuromuscular diseases--a world survey. Neuromuscul Disord. 1991;1(1):19-29.

3. Lapidos KA, Kakkar R, McNally EM. The dystrophin glycoprotein complex: signaling strength and integrity for the sarcolemma. Circ Res. 2004;94(8):1023-31.

4. Finsterer J. Cardiopulmonary support in duchenne muscular dystrophy. Lung. 2006;184(4):205-15.

5. Swiderski K, Lynch GS. Murine models of Duchenne muscular dystrophy: is there a best model? Am J Physiol Cell Physiol. 2021;321(2):C409-C12.

6. Hammers DW, Hart CC, Matheny MK, Wright LA, Armellini M, Barton ER, Sweeney HL. The D2.mdx mouse as a preclinical model of the skeletal muscle pathology associated with Duchenne muscular dystrophy. Sci Rep. 2020;10(1):14070.

7. Marshall JL, Crosbie-Watson RH. Sarcospan: a small protein with large potential for Duchenne muscular dystrophy. Skelet Muscle. 2013;3(1):1.

8. Shu C, Parfenova L, Mokhonova E, Collado JR, Damoiseaux R, Campagna J, et al. High-throughput screening identifies modulators of sarcospan that stabilize muscle cells and exhibit activity in the mouse model of Duchenne muscular dystrophy. Skelet Muscle. 2020;10(1):26.

9. Gibbs EM, McCourt JL, Shin KM, Hammond KG, Marshall JL, Crosbie RH. Loss of sarcospan exacerbates pathology in mdx mice, but does not affect utrophin amelioration of disease. Hum Mol Genet. 2021;30(3-4):149-59.

10. Stearns-Reider KM, Hicks MR, Hammond KG, Reynolds JC, Maity A, Kurmangaliyev YZ, et al. Myoscaffolds reveal laminin scarring is detrimental for stem cell function while sarcospan induces compensatory fibrosis. NPJ Regen Med. 2023;8(1):16.

11. Metzger T, Gache V, Xu M, Cadot B, Folker ES, Richardson BE, et al. MAP and kinesin-dependent nuclear positioning is required for skeletal muscle function. Nature. 2012;484(7392):120-4.

12. Weller B, Karpati G, Carpenter S. Dystrophin-deficient mdx muscle fibers are preferentially vulnerable to necrosis induced by experimental lengthening contractions. J Neurol Sci. 1990;100(1-2):9-13.

13. Gibbs EM, Marshall JL, Ma E, Nguyen TM, Hong G, Lam JS, et al. High levels of sarcospan are well tolerated and act as a sarcolemmal stabilizer to address skeletal muscle and pulmonary dysfunction in DMD. Hum Mol Genet. 2016;25(24):5395-406.

14. van Putten M, Putker K, Overzier M, Adamzek WA, Pasteuning-Vuhman S, Plomp JJ, Aartsma-Rus A. Natural disease history of the D2-mdx mouse model for Duchenne muscular dystrophy. FASEB J. 2019;33(7):8110-24.

15. Mamsa H, Stark RL, Shin KM, Beedle AM, Crosbie RH. Sarcospan increases laminin-binding capacity of alpha-dystroglycan to ameliorate DMD independent of Galgt2. Hum Mol Genet. 2022;31(5):718-32.

16. Ceco E, McNally EM. Modifying muscular dystrophy through transforming growth factor-beta. FEBS J. 2013;280(17):4198-209.

17. Tinsley JM, Blake DJ, Roche A, Fairbrother U, Riss J, Byth BC, et al. Primary structure of dystrophin-related protein. Nature. 1992;360(6404):591-3.

18. von der Mark H, Durr J, Sonnenberg A, von der Mark K, Deutzmann R, Goodman SL. Skeletal myoblasts utilize a novel beta 1-series integrin and not alpha 6 beta 1 for binding to the E8 and T8 fragments of laminin. J Biol Chem. 1991;266(35):23593-601.

19. Song WK, Wang W, Foster RF, Bielser DA, Kaufman SJ. H36-alpha 7 is a novel integrin alpha chain that is developmentally regulated during skeletal myogenesis. J Cell Biol. 1992;117(3):643-57.

20. Deconinck AE, Potter AC, Tinsley JM, Wood SJ, Vater R, Young C, et al. Postsynaptic abnormalities at the neuromuscular junctions of utrophin-deficient mice. J Cell Biol. 1997;136(4):883-94.

21. Ciafaloni E, Fox DJ, Pandya S, Westfield CP, Puzhankara S, Romitti PA, et al. Delayed diagnosis in duchenne muscular dystrophy: data from the Muscular Dystrophy Surveillance, Tracking, and Research Network (MD STARnet). J Pediatr. 2009;155(3):380-5.

22. Heydemann A, Ceco E, Lim JE, Hadhazy M, Ryder P, Moran JL, et al. Latent TGF-beta-binding protein 4 modifies muscular dystrophy in mice. J Clin Invest. 2009;119(12):3703-12.

23. Pratt JM, Simpson DM, Doherty MK, Rivers J, Gaskell SJ, Beynon RJ. Multiplexed absolute quantification for proteomics using concatenated signature peptides encoded by QconCAT genes. Nat Protoc. 2006;1(2):1029-43.

24. Bella J, Hulmes DJ. Fibrillar Collagens. Subcell Biochem. 2017;82:457-90.

25. Shaw LM, Olsen BR. FACIT collagens: diverse molecular bridges in extracellular matrices. Trends Biochem Sci. 1991;16(5):191-4.

26. Hirst RC, McCullagh KJ, Davies KE. Utrophin upregulation in Duchenne muscular dystrophy. Acta Myol. 2005;24(3):209-16.